



Effect of oxygen and sodium sulfide on flotation of cuprite and its modification mechanism

Xiao-dong JIA^{1,2}, Kai-wei SONG^{1,2}, Jin-peng CAI^{1,2},
Chao SU^{1,2}, Xiao-hui XU³, Yin-yu MA⁴, Pei-lun SHEN^{1,2}, Dian-wen LIU^{1,2}

1. State Key Laboratory of Complex Nonferrous Metal Resources Clean Utilization, Kunming University of Science and Technology, Kunming 650093, China;
2. Yunnan Key Laboratory of Green Separation and Enrichment of Strategic Mineral Resources, Kunming University of Science and Technology, Kunming 650093, China;
3. Graduate School, North China University of Science and Technology, Tangshan 063210, China;
4. Shandong Gold Group Co., Ltd., Jinan 250100, China

Received 12 December 2021; accepted 7 March 2022

Abstract: Effect of oxygen and Na₂S on the flotation of cuprite was investigated by flotation test, FESEM, EMPA and XPS. The micro-flotation experiments indicated that the flotation recovery of cuprite can be greatly increased by adding an appropriate amount of Na₂S. FESEM showed that numerous fragments were covered on the cuprite surfaces after sulfidization, and the shapes of these fragments were more regular and complete with the Na₂S concentration of 5.0×10⁻⁴ mol/L. EPMA and EDS analysis confirmed that these fragments were newly-formed copper sulfide species, which was the key to promoting the flotation of cuprite. XPS analysis revealed that the sulfidization process of cuprite was that Na₂S first underwent an oxidation–reduction reaction with the CuO on its surface, which was due to the extremely easy oxidation of the surface of cuprite. The Cu²⁺ was reduced to Cu⁺, and S²⁻ was mainly oxidized to (S₂)²⁻ and (S_n)²⁻.

Key words: cuprite; sulfidization flotation; sulfidization mechanism; oxidization; copper sulfide species

1 Introduction

Cuprite (Cu₂O), a copper oxide mineral with commercial economic value, generally forms in the oxidation zone of copper rich ore deposits [1]. The hydrometallurgical treatment of copper oxide ore to recover copper is a method characterized by a relatively high extraction rate and low cost [2,3]. However, the acid leaching method is not applicable to cuprite, due to the disproportionation of cuprous copper ions (Cu⁺) under acidic conditions, and the theoretical maximum extraction rate can only reach 50% [4]. In solutions with oxidizing environments, ammonium molecules can

complex cuprous and cupric copper ions without precipitating; hence, ammonium leaching is a feasible technical route for cuprite extraction [4,5]. However, the application of this method is limited to a certain extent due to the instability of ammonium, its corrosiveness to equipment, and environmental pollution [3,6].

In industry applications, froth flotation is one of the main methods for the recovery of copper oxide minerals. Compared with copper sulfide minerals, the surfaces of copper oxide minerals are more hydrophilic and soluble, so they cannot be directly floated with a conventional sulfide minerals collector [7–10]. Therefore, it is a common practice to sulfidize copper oxide minerals before flotation

via the addition of a sulfidizing reagent to the pulp [11]. HEYES and TRAHAR [12] found that cuprite treated with sodium sulfide (Na_2S) exhibited good floatability. Compared with mechanochemical, hydrothermal, and roasting methods, the method of directly adding a sulfidizing agent into the pulp (surface sulfidization) is characterized by low cost, simplicity of operation, and low corrosion of the equipment [13]. As the most common sulfidizing reagent, Na_2S supplies sulfide species for oxide mineral. The amount of Na_2S must be strictly controlled, because excessive sulfur species will significantly inhibit the absorption of the collector on the surface of the mineral particles [14,15]. Hydrolysis equilibrium exists in Na_2S solution, and, according to thermodynamic calculation, the distribution of sulfide species depends on the pH of the solution. The dominant sulfide species in aqueous Na_2S solution are H_2S at $\text{pH}<7.0$, HS^- at $\text{pH}=7.0\text{--}13.9$, and S^{2-} at $\text{pH}>13.9$ [16,17]. According to previous research, the optimal flotation recovery of the sulfide–xanthate flotation of copper oxide minerals is obtained under mild alkaline conditions; thus, it can be inferred that HS^- plays a major role in sulfidization [6,18,19].

The sulfidization process of copper oxide minerals is complicated, and is generally considered to comprise the adsorption of sulfide species on the surface, sulfide oxidation, and the desorption of oxidized compounds according to the ion-exchange reaction [20–22]. In early researches, limited by the lack of characterization methods, it was generally believed that the sulfide thin film on the surfaces of copper oxide minerals was chalcocite (Cu_2S). With the development and progression of detection technology, the sulfide products on the surfaces of copper oxide minerals have been more accurately characterized. XPS analysis conducted by FENG et al [16] and WU et al [23] indicated that sulfide products formed on malachite surfaces comprised monosulfide, disulfide, and polysulfide. Via the utilization of the different dissolution behaviors of malachite and copper sulfide in sulfuric acid, the sulfide product on the surface of malachite was extracted and its crystal phase was confirmed [21]. Under the condition of the optimal Na_2S dosage, the sulfurized products on the malachite surface were found to comprise djurleite ($\text{Cu}_{31}\text{S}_{16}$) and anilite (Cu_7S_4). However, there have been few studies on the surface properties of cuprite and the mechanism

of sulfidization flotation.

Thus, we believe that the sulfidization–xanthate flotation on cuprite is still a valuable method for use in the future. In this study, the effect of oxygen and sodium sulfide on the flotation of cuprite and its activation mechanism were investigated.

2 Experimental

2.1 Materials and reagents

The cuprite samples obtained from Guangxi, China, were crushed using a hammer, and a laboratory double-roll crusher was then used for further crushing. The gangue and impurities visible to the naked eye were then removed manually. Chemical analysis revealed that 87.9% Cu was present in the mineral, and XRD analysis (Fig. 1) indicated that only a pure cuprite diffraction peak was detected. Finally, an agate mortar was used to dry-grind the cuprite sample, and the particle size was controlled between 0.074 and 0.038 mm with a Tyler sieve.

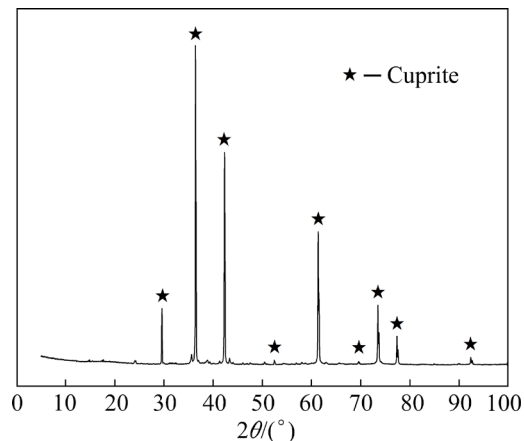


Fig. 1 X-ray diffraction pattern of pure cuprite samples

In this work, sodium sulfide ($\text{Na}_2\text{S}\cdot 9\text{H}_2\text{O}$, AR grade) was utilized as the sulfidizing reagent, and the purified industrial-grade sodium butyl xanthate (NaBX , $\text{C}_4\text{H}_9\text{OCSSNa}$) served as the collector for floating cuprite. Both were prepared into a solution of 5×10^{-4} mol/L concentration for use. Sodium hydroxide (NaOH , AR grade) and hydrochloric acid (HCl , AR grade) were employed as pH value regulators, and were prepared into a stock solution of 0.1 mol/L for use. Deionized water, which was prepared using a Mill-Q50 water-purifying device made in the United States, was used in all the

experiments, and fresh chemical solutions were prepared daily.

2.2 Micro-flotation tests

To investigate sulfidization–flotation behavior of cuprite, micro-flotation experiments were performed in a 50 mL Hallimond tube at ambient temperature. For each test, 0.5 g of pure cuprite and 50 mL of deionized water were placed into a beaker and then stirred with an electric mechanical agitator for 1 min. Then, 0.1 mol/L NaOH and 0.1 mol/L H₂SO₄ stock solutions were employed to regulate the pH of the pulp. A certain amount of reagent solution was added into the pulp according to the requirements of the experimental design, and the reaction time for each reagent was 3 min. Afterward, the suspension was quickly transferred into the Hallimond tube, which was inflated with nitrogen gas at a rate of 40 mL/min, and the flotation time was 5 min. After completing the flotation tests, the froth products and tailings were collected, dried, and weighed, and the recovery was calculated by the mass fraction of the froth products. Each set of micro-flotation tests was conducted three times, and the average flotation recovery and standard deviation were calculated and plotted.

2.3 FESEM–EDS and XPS analysis

The sample processing was as follows. First, 0.5 g of the cuprite sample and 50 mL of deionized water were stirred with an electric mechanical agitator in a beaker for 1 min, and a specified amount of Na₂S solution was added to the pulp. After 3 min of sulfidizing treatment, the supernatant was removed, and the treated cuprite samples were cleaned with deionized water several times and then dried in a vacuum drying chamber. Then, FESEM (Nova NanoSEM450) was conducted to characterize the surface micro-topographies of the treated cuprite samples, EDS (Oxford X-Max) and XPS were then employed to analyze the chemical compositions and elements on the surfaces of the treated cuprite samples.

The equipment used was as follows.

Before FESEM and EDS detection, all samples were sprayed with platinum (Pt) metal to enhance the conductivity of the cuprite surfaces.

The XPS data were obtained using a PHI5000 Versaprobe-II (Ulvac-Phi, Japan) scanning XPS microprobe system with a monochromatized Al K_α

X-ray source (1486.6 eV). The survey scans were conducted at a pass energy of 46.95 eV, and multiplex high-resolution scans were recorded at 30 eV. The resulting spectra were charge-corrected using C 1s at a binding energy of 284.8 eV. Data processing and fitting were conducted using MultiPak software.

2.4 EPMA analysis

EPMA was performed with the use of an EPMA-1720 series device (Shimadzu Corporation) equipped with four wavelength-dispersive spectrometer (WDS) detectors to characterize the distributions of oxygen, sulfur, and copper on the surfaces of the sulfidized cuprite samples.

0.5 g of the sulfidized cuprite sample was solidified in a mold with epoxy resin and curing agent for 12 h, and was then polished with emery paper to expose the fresh mineral surface. Then, the polished samples were washed with deionized water and dried in a vacuum drying chamber at 30 °C. The samples were then coated with carbon before measurement.

3 Results and discussion

3.1 Micro-flotation

Figure 2 presents the flotation recovery of cuprite as a function of the NaBX concentration in the absence or presence of Na₂S. With the increase of the NaBX concentration, the flotation recovery of cuprite in both the absence and presence of Na₂S was increased. The floatability of the cuprite samples treated with 1.0×10^{-4} mol/L Na₂S solution

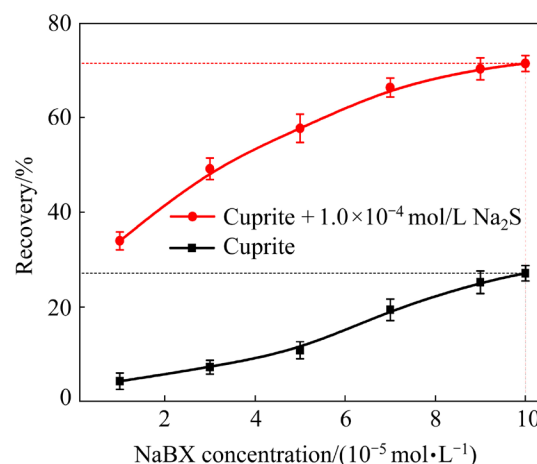


Fig. 2 Flotation recovery of cuprite as function of concentration of NaBX in the absence and presence of 1.0×10^{-4} mol/L Na₂S at pH=9.0

was significantly higher than that of unsulfidized cuprite samples. These findings indicate that sulfidization could significantly improve the floatability of cuprite.

According to previous research and experience, an appropriate amount of Na_2S is a crucial factor for the flotation of copper oxide minerals. The floatability of cuprite as a function of the Na_2S concentration at a fixed NaBX concentration is presented in Fig. 3. The results indicate that the flotation recovery of cuprite increased greatly with the increase of Na_2S concentration until it reached around 1.0×10^{-4} mol/L. Then, the floatability of cuprite decreased sharply, and the maximum flotation recovery was attained at the Na_2S concentration of 1.0×10^{-4} mol/L. The results show that an appropriate amount of Na_2S can significantly improve the floatability of cuprite, while excessive Na_2S can inhibit its floatability, which is consistent with previous research [7,11,24]. The cuprite samples treated with excessive Na_2S exhibited good floatability again after washing, indicating that the inhibition was caused by excessive sulfur ion species in the solution.

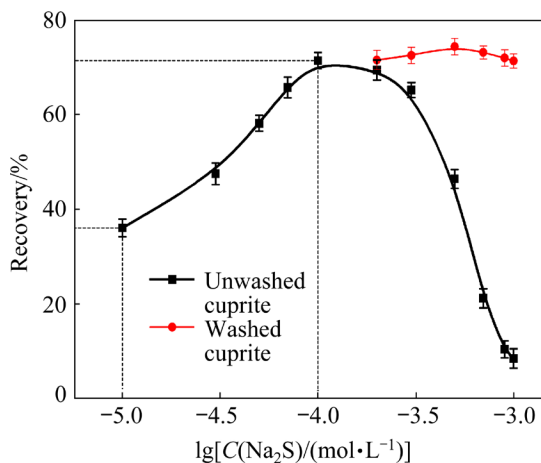


Fig. 3 Flotation recovery of washed and unwashed cuprite with 1.0×10^{-4} mol/L NaBX as function of concentration of Na_2S at $\text{pH}=9.0$

Figure 4 presents the flotation recovery of cuprite treated with Na_2S as a function of the pH . The results show that the acidity and alkalinity of the pulp had a significant effect on the sulfidization effect of the cuprite, and the maximum flotation recovery was obtained at $\text{pH}=9.0$. According to the hydrolysis equilibrium of Na_2S in the solution, the sulfur ion species in the solution at $\text{pH}=9.0$ were mainly HS^- , and it can therefore be inferred that

HS^- plays a major role in the sulfidization of cuprite.

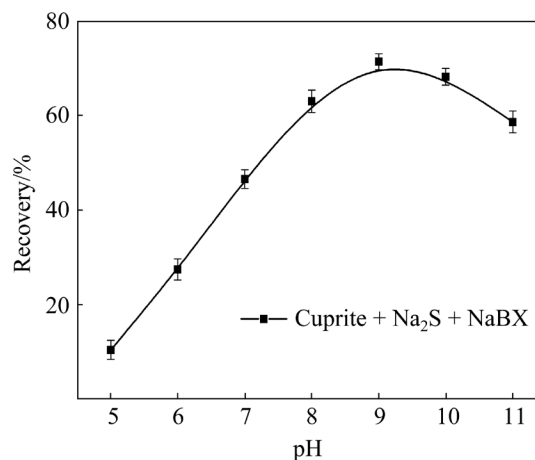


Fig. 4 Flotation recovery of cuprite with 1.0×10^{-4} mol/L NaBX and Na_2S as function of pH

The preceding investigations showed that an appropriate amount of Na_2S is beneficial to the flotation of cuprite, though the sulfidization mechanism is not yet clear. Thus, the subsequent study is focused on the activation mechanism of the effect of Na_2S on cuprite flotation.

3.2 FESEM–EDS results

Figures 5(a) and 6(a₃, a₄) present the surface microtopographies of raw cuprite and its EDS images, respectively. The results of FESEM–EDS reveal that the cuprite sample was very pure and only contained Cu and O, and the microscopic surface of the cuprite was not smooth.

Figure 5(b) presents the surface microtopography of cuprite treated with 1.0×10^{-4} mol/L Na_2S solution at different magnifications. At relatively low magnification, as shown in Figs. 5(b₁) and 5(b₂), no significant variation of the microtopography was observed. At higher magnifications, it was found that many regular fragments were formed on the cuprite surface. Additionally, as given in Table 1, the presence of sulfur was detected by EDS and the sulfur contents of Points 1, 2, and 3 were respectively 1.5, 1.1 and 1.3 (wt.%), indicating that the surface of the cuprite was covered with one or more layers of hydrophobic copper sulfide species. This is the main reason for the achievement of the good flotation recovery of cuprite. With the addition of excessive Na_2S solution, the micro-flotation experiments showed that the flotation of cuprite

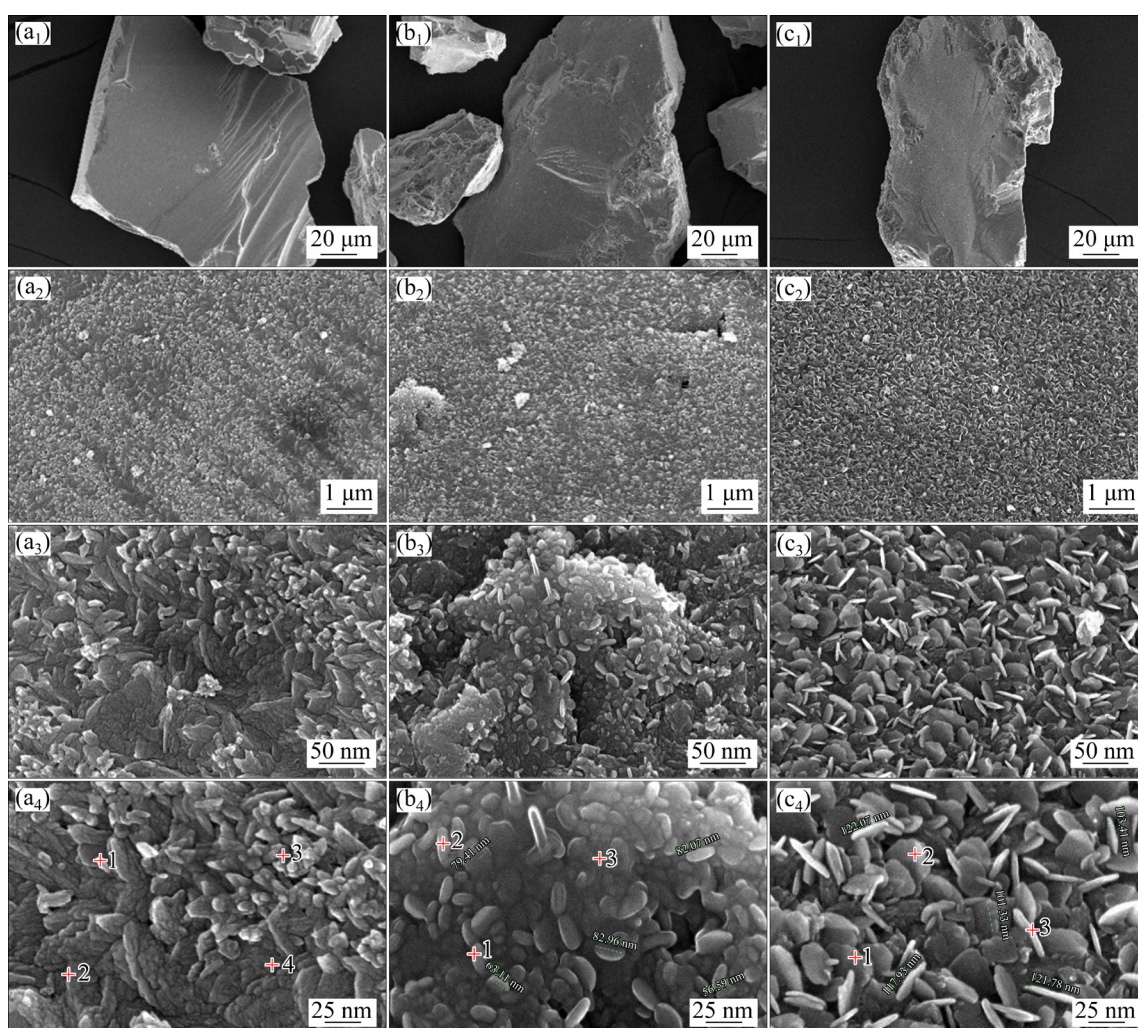


Fig. 5 FESEM images of surface microtopographs of raw cuprite (a), cuprite treated with 1.0×10^{-4} mol/L Na_2S (b), and cuprite treated with 5.0×10^{-4} mol/L Na_2S (c)

was depressed. However, the FESEM and EDS test results were contrary to the flotation behavior of cuprite. It can be seen from Fig. 5(c) that a denser copper sulfide film was formed on the surface of the cuprite, and the shapes of these copper sulfide crystals were more regular and complete. The EDS results presented in Fig. 6(c₄) and Table 1 also confirm that the sulfur content was greater than that under the condition of 1.0×10^{-4} mol/L Na_2S . Combined with the micro-flotation test results, it was confirmed that the reason why the flotation of cuprite was promoted is that many copper sulfide species were formed on its surface, while the reason why excessive Na_2S depressed the flotation of cuprite was mainly in the solution. Therefore, the key to obtaining a better flotation recovery of cuprite is the control of the amount of sulfidizing agent.

3.3 EPMA results

FESEM–EDS analysis revealed that numerous uniform fragments were formed on the surface of the cuprite treated with Na_2S solution. However, a limitation of FESEM is that only a partial morphology can be observed when the magnification becomes too high. In contrast, the application of EPMA can characterize the distributions of sulfur on the surfaces of multiple cuprite particles, and is therefore an important supplement to FESEM analysis.

Figure 7(a) presents the mapping results of S, Cu, and O on the cuprite surfaces. Because the cuprite composition did not contain sulfur, the sulfur distributed on the cuprite surface shown in Fig. 7(a₁) was reasonable. Figures 7(a₂, a₃) present the distributions of Cu and O, respectively, on the cuprite surface, which were found to be uneven. It

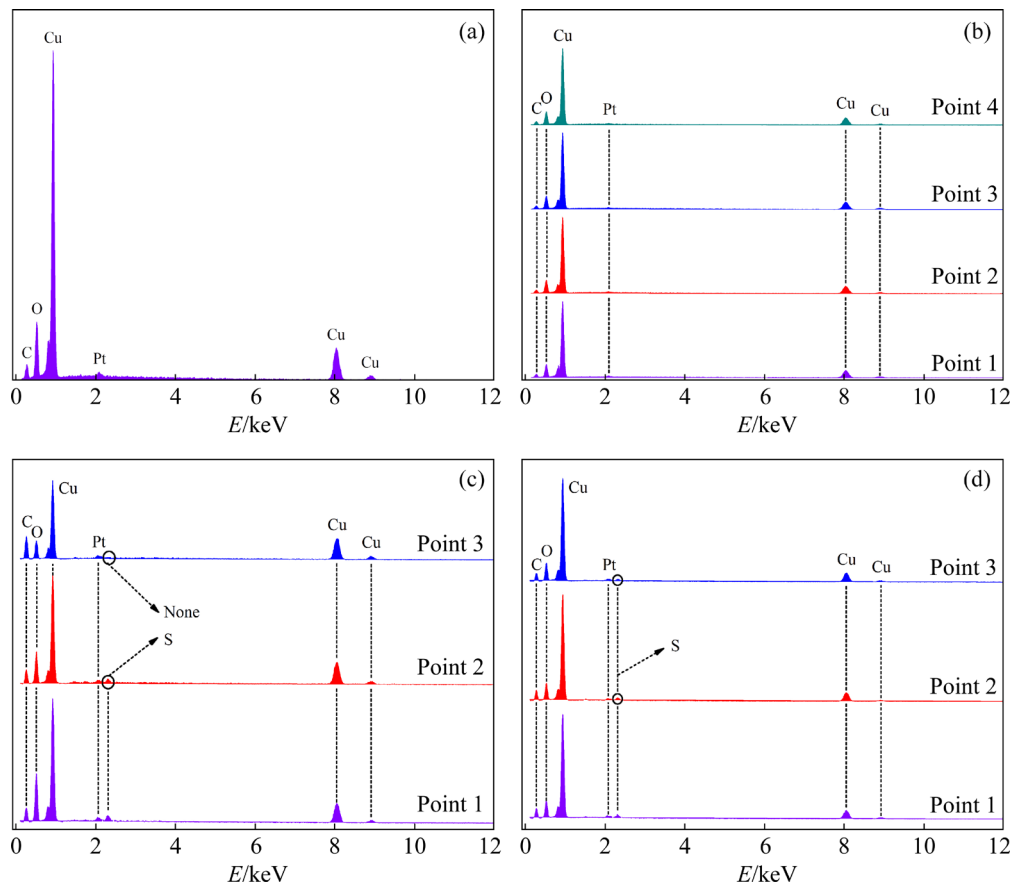


Fig. 6 EDS results corresponding to Figs. 5(a₃) (a), 5(a₄) (b), 5(b₄) (c), and 5(c₄) (d)

Table 1 Contents of O, Cu, and S for points in Fig. 5 (wt.%)

Element	Fig. 5(a ₃)		Fig. 5(a ₄)			Fig. 5(b ₄)			Fig. 5(c ₄)		
	Plane	Point 1	Point 2	Point 3	Point 4	Point 1	Point 2	Point 3	Point 1	Point 2	Point 3
O	12.3	13.1	11.8	12.3	12.1	11.8	12.6	12.0	12.6	12.2	10.8
Cu	87.7	86.9	88.2	87.7	87.9	86.7	86.3	86.7	85.2	85.8	86.8
S	0.0	0.0	0.0	0.0	0.0	1.5	1.1	1.3	2.2	2.0	2.4

was found that some particles in the Figs. 7(a₂, a₃) have uneven element distribution on the surface. For example, the Cu content at Position 2 was higher than that at Position 1, and, correspondingly, the O content at Position 2 was lower than that at Position 1. This is because, during the processing of the pure cuprite sample, the fresh cuprite surface was exposed after the Position 1 was polished, while Position 2 was not polished. In other words, Position 1 represents the surface of cuprite (88.8% Cu; 11.2% O), and Position 2 represents the surface of tenorite (79.89% Cu; 20.11% O), which is related to the easy oxidation of the cuprite. In fact, the cuprite was covered with a CuO film before the sulfidization reaction occurred.

Figure 7(b) presents the mapping results of S, Cu, and O on the sulfidized cuprite surfaces. Figure 7(b₁) reveals that the surface of the sulfidized cuprite was covered with sulfur, indicating that one or more layers of hydrophobic copper sulfide film were indeed formed on the cuprite surface after the sulfidization, which is consistent with the results of FESEM–EDS. Moreover, a phenomenon similar to that presented in Figs. 7(a₂, a₃) can be observed in Figs. 7(b₂, b₃), i.e., the Cu and O were unevenly distributed on the surface of the same cuprite particle. Position 2 in Fig. 7(b) also represents the surface of cuprite, while Position 1 represents copper sulfide species. The reason why the O content at Position 1 was higher than that at Position

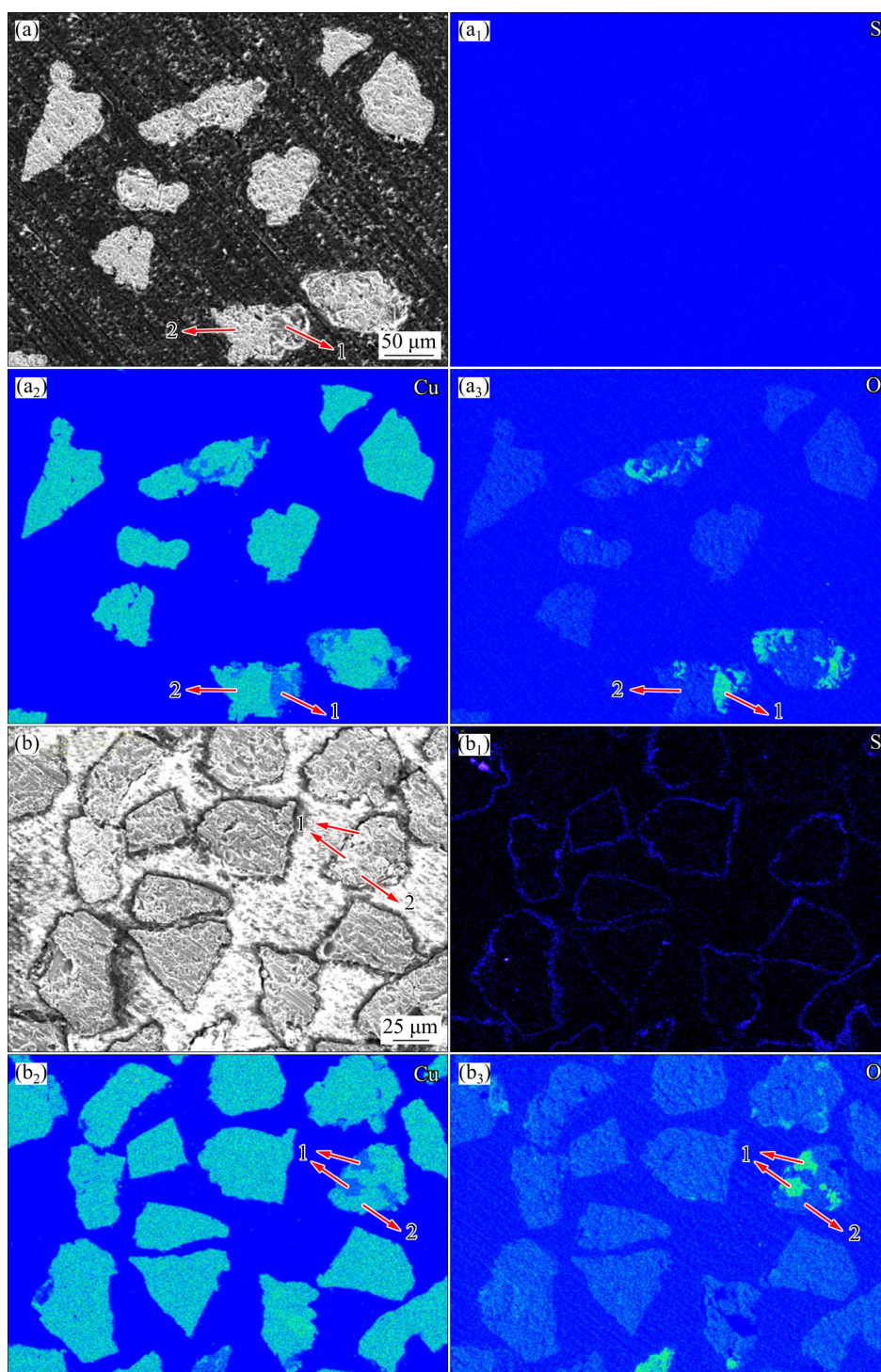


Fig. 7 EPMA mappings of pure cuprite (a) and cuprite treated with 5.0×10^{-4} mol/L Na_2S (b)

2 was that the copper sulfide species at Position 1 exhibited oxidation behavior, e.g., SO_4^{2-} , which led to the enrichment of O at this position.

3.4 XPS results

The EPMA measurements showed that the cuprite surface was easily oxidized to CuO when exposed to air, and the Na_2S was likely to first react

with the CuO in the outermost layer and then with the Cu_2O in the inner layer. Thus, XPS was employed to further confirm this result.

For all the cases, peak-fitting for the Cu 2p and S 2p line shapes was performed using a Gaussian–Lorentzian product function with the spin-orbit splitting of 19.90 and 1.18 eV and an intensity ratio $I(2p_{3/2}): I(2p_{1/2})$ of 2:1 [25–27].

Figures 8(a₁, b₁, c₁) present the O 1s XPS core-level spectra of oxide elements on the sulfidized and unsulfidized cuprite surfaces. As is evident from visual inspection, the peak fittings of the O 1s spectra in Figs. 8(a₁, b₁, c₁) reveal the presence of two well-defined doublets with the binding energies of 529.9 and 531.4, 530.2 and 531.7 eV, and 530.0 and 531.7 eV, respectively. The binding energy of 529.9 eV in Fig. 8(a₁) represents the O²⁻ in CuO, indicating that the surface of cuprite was indeed covered with a CuO thin film, which was gradually consumed as the sulfidization reaction progressed. The data in Table 2 indicate that the content of O²⁻ in CuO decreased from 54.06% to 18.38% and to 3.45%, which provides direct evidence for the preceding statement. In contrast, the content of O²⁻ in Cu₂O and OH⁻ increased from 45.94% to 81.62% and to

96.55%, which also indicates that the CuO film was involved in the sulfidization reaction [28]. Thus, it can be concluded that the Na₂S first reacted with the outermost CuO, and then reacted with the inner Cu₂O.

Figures 8(a₂, b₂, c₂) present the Cu 2p XPS core-level spectra of the Cu element on the sulfidized and unsulfidized cuprite surfaces. First, it is evident that the spectrum in Fig. 8(a₂) has a strong Cu(II) satellite “shake-up” peak at approximately 940–945 eV [29–31], which once again provides a direct evidence of the CuO film covering the surface of the cuprite (Cu₂O). As the sulfidization occurred, the Cu 2p fitting peaks in Figs. 8(b₂, c₂) show that the area of the Cu(II) satellite peak gradually decreased with the increase of the dosage of Na₂S, which indicates that the Cu(II) on the cuprite surface was consumed by the

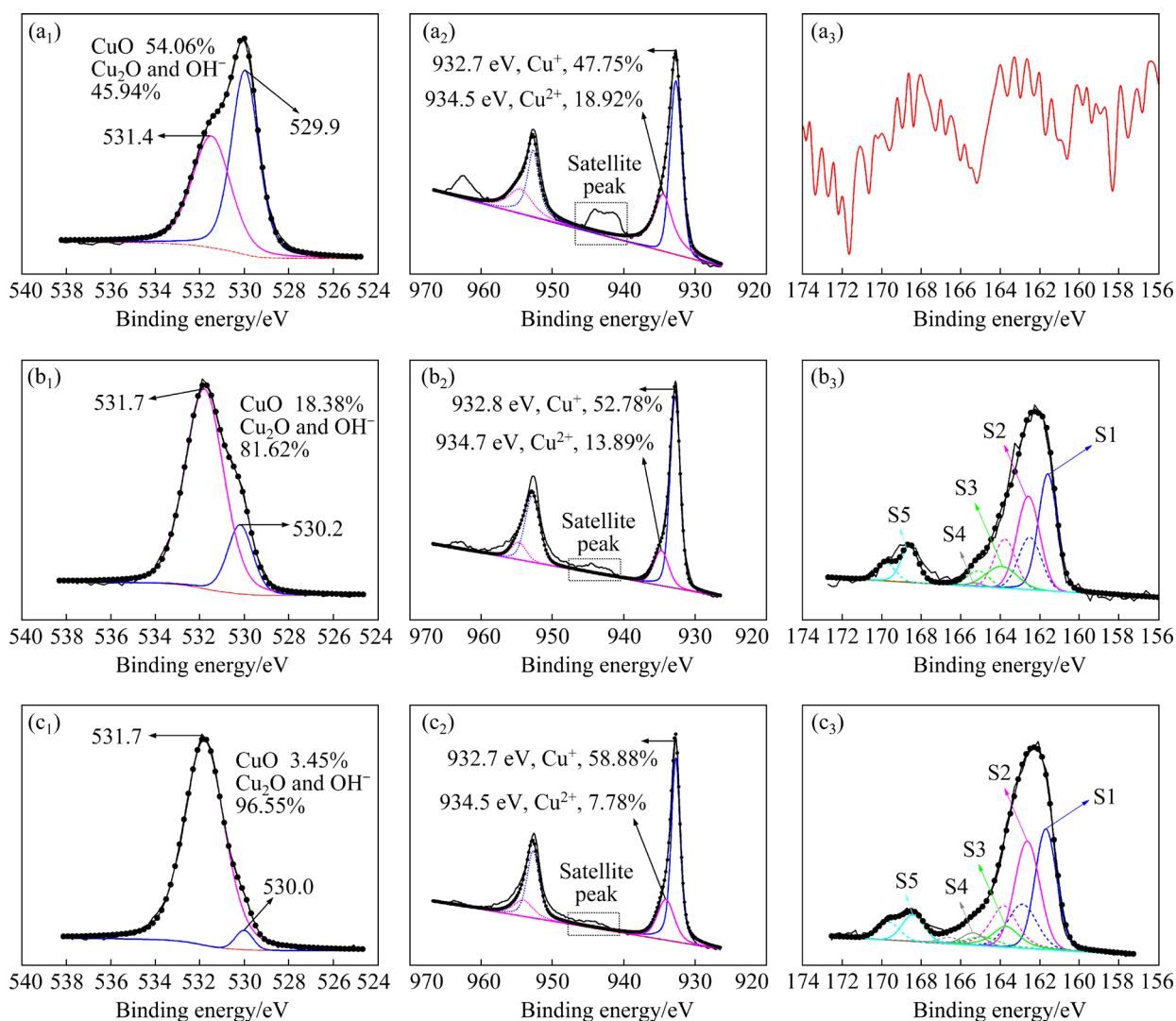


Fig. 8 O 1s, Cu 2p, and S 2p XPS core-level spectra: (a) Raw cuprite; (b) Cuprite treated with 1.0×10^{-4} mol/L Na₂S; (c) Cuprite treated with 5.0×10^{-4} mol/L Na₂S

Table 2 Peak parameters employed in peak-fitting of photoemission spectra of cuprite surfaces

Core level	Figure	Binding energy/eV	Species	Spin-orbit splitting/eV	Percentage/%
O 1s	8(a ₁)	529.9	O ²⁻ in CuO	None	54.06
		531.4	O ²⁻ in Cu ₂ O and OH ⁻		45.94
	8(b ₁)	530.2	O ²⁻ in CuO	None	18.38
		531.7	O ²⁻ in Cu ₂ O and OH ⁻		81.62
	8(c ₁)	530.0	O ²⁻ in CuO	None	3.45
		531.7	O ²⁻ in Cu ₂ O and OH ⁻		96.55
Cu 2p _{2/3}	8(a ₂)	932.7	Cu ⁺ in Cu ₂ O and Cu _x S _y	19.90	47.75
		934.5	Cu ²⁺ in CuO		18.92
	8(b ₂)	932.8	Cu ⁺ in Cu ₂ O and Cu _x S _y	19.90	52.78
		934.7	Cu ²⁺ in CuO		13.89
	8(c ₂)	932.7	Cu ⁺ in Cu ₂ O and Cu _x S _y	19.90	58.88
		934.5	Cu ²⁺ in CuO		7.78
S 2p _{2/3}	8(a ₃)	–	–	–	–
	8(b ₃ , c ₃)	S1: 161.4	S ²⁻	1.18	100
		S2: 162.8	(S ₂) ²⁻		
		S3: 163.7	(S _n) ²⁻		
		S4: 165.3	S ₀		
		S5: 168.4	(SO ₄) ²⁻		

sulfidization reaction. This is consistent with the results reported in Table 2, which reveals that the content of Cu²⁺ in CuO decreased from 18.92% to 13.89% and to 7.78%. Secondly, the binding energies of 932.7, 932.8, and 932.7 eV were due to the Cu(I) on the mineral surface [27]. For the raw pure cuprite, the Cu(I) fitting peak is contributed by two parts; the first part originated from the Cu(I) contained in the cuprite itself, and the other part originated from the reduction of Cu(II) in CuO.

Figures 8(a₃, b₃, c₃) present the S 2p XPS core-level spectra of the S element on the surfaces of the sulfidized and unsulfidized cuprite. The S 2p fitting peak in Fig. 8(a₃) is disorganized, which is consistent with the fact that the cuprite itself does not contain any S element. Additionally, the S 2p fitting peaks in Figs. 8(b₃, c₃) are basically the same, suggesting that the S species were the same under the conditions of 1.0×10⁻⁴ mol/L and 5.0×10⁻⁴ mol/L Na₂S. Therefore, Fig. 8(c₃) was taken as an example to analyze the changes in the valence state of S.

The binding energies of S1 2p_{3/2}, S2 2p_{3/2}, S3 2p_{3/2}, S4 2p_{3/2}, and S5 2p_{3/2} were respectively located at 161.4, 162.8, 163.7, 165.3 and 168.4 eV, which correspond to S²⁻, (S₂)²⁻, (S_n)²⁻, S₀, and (SO₄)²⁻ [32–35]. The presence of high-valence S species, such as (S₂)²⁻, (S_n)²⁻, S₀, and (SO₄)²⁻, on

the sulfidized cuprite surface indicates that an oxidation–reduction reaction occurred between Cu²⁺ and S²⁻, and the negative divalent sulfur conformed to the law of gradual oxidation from a low valence state to a high valence state. The presence of S²⁻ confirms that, in addition to the oxidation–reduction reaction, a substitution reaction also occurred on the cuprite surface, which also corresponds to the XPS analysis results of Cu.

4 Conclusions

(1) The use of Na₂S as an activator can greatly promote the xanthate flotation of cuprite, due to the hydrophobic copper sulfide species formed on its surface. However, excessive Na₂S solution can seriously depress the cuprite flotation due to the copper sulfide colloid formed in the solution.

(2) The cuprite was found to be easily oxidized when exposed to air, and its surface was covered by more stable CuO. The sulfidization process of cuprite is that Na₂S first undergoes an oxidation–reduction reaction with CuO on its surface, and a substitution reaction then occurs between the cuprite and Na₂S as the depth of the reaction changes.

(3) During the oxidation–reduction reaction between CuO and Na₂S, the Cu²⁺ ions are reduced

to Cu^+ , while the S^{2-} ions are mainly oxidized to $(\text{S}_2)^{2-}$ and $(\text{S}_n)^{2-}$.

Acknowledgments

This research was supported by the National Natural Science Foundation of China (No. 52074138), and the Fundamental Research Project of Yunnan Province, China (No. 202001AS070030).

References

- [1] BUCKLEY A N, GOH S W, SKINNER W M, WOODS R, FAN L J. Interaction of cuprite with dialkyl dithiophosphates [J]. *International Journal of Mineral Processing*, 2009, 93(2): 155–164.
- [2] OSSEO-ASARE K, FUERSTENAU D W. Adsorption phenomena in hydrometallurgy. 1: The uptake of copper, nickel and cobalt by oxide adsorbents in aqueous ammoniacal solutions [J]. *International Journal of Mineral Processing*, 1979, 6(2): 85–104.
- [3] PEACEY J, GUO Xian-jian, ROBLES E. Copper hydrometallurgy—Current status, preliminary economics, future direction and positioning versus smelting [J]. *Transactions of Nonferrous Metals Society of China*, 2004, 14(3): 560–568.
- [4] ARACENA A, PÉREZ F, CARVAJAL D. Leaching of cuprite through NH_4OH in basic systems [J]. *Transactions of Nonferrous Metals Society of China*, 2018, 28(12): 2545–2552.
- [5] TANDA B C, EKSTEEN J J, ORABY E A. An investigation into the leaching behaviour of copper oxide minerals in aqueous alkaline glycine solutions [J]. *Hydrometallurgy*, 2017, 167: 153–162.
- [6] SHEN Pei-lun, LIU Dian-wen, ZHANG Xiao-lin, JIA Xiao-dong, SONG Kai-wei, LIU Dan. Effect of $(\text{NH}_4)_2\text{SO}_4$ on eliminating the depression of excess sulfide ions in the sulfidization flotation of malachite [J]. *Minerals Engineering*, 2019, 137: 43–52.
- [7] CAI Jin-peng, SHEN Pei-lun, LIU Dian-wen, ZHANG Xiao-lin, FANG Jian-jun, SU Chao, YU Xing-cai, LI Jiang-li, WANG Han. Growth of covellite crystal onto azurite surface during sulfurization and its response to flotation behavior [J]. *International Journal of Mining Science and Technology*, 2021, 31: 1003–1012.
- [8] LI Fang-xu, ZHOU Xiao-tong, LIN Ri-xiao. Flotation performance and adsorption mechanism of novel 1-(2-hydroxyphenyl)hex-2-en-1-one oxime flotation collector to malachite [J]. *Transactions of Nonferrous Metals Society of China*, 2020, 30: 2792–2801.
- [9] SHEN Pei-lun, LIU Dian-wen, XU Xiao-hui, JIA Xiao-dong, ZHANG Xiao-lin, SONG Kai-wei, CAI Jin-peng. Effects of ammonium phosphate on the formation of crystal copper sulfide on chrysocolla surfaces and its response to flotation [J]. *Minerals Engineering*, 2020, 155: 106300.
- [10] CHEN Jian-hua. The interaction of flotation reagents with metal ions in mineral surfaces: A perspective from coordination chemistry [J]. *Minerals Engineering*, 2021, 171: 107067.
- [11] CORIN K C, KALICHINI M, O'CONNOR C T, SIMUKANGA S. The recovery of oxide copper minerals from a complex copper ore by sulphidisation [J]. *Minerals Engineering*, 2017, 102: 15–17.
- [12] HEYES G W, TRAHAR W J. Oxidation–reduction effects in the flotation of chalcocite and cuprite [J]. *International Journal of Mineral Processing*, 1979, 6(3): 229–252.
- [13] LIU Rui-zeng, LIU Dian-wen, LI Jia-lei, LIU Si-yan, LIU Zhi-cheng, GAO Lian-qi, JIA Xiao-dong, AO Shun-fu. Improved understanding of the sulfidization mechanism in cerussite flotation: An XPS, ToF-SIMS and FESEM investigation [J]. *Colloids and Surfaces A: Physicochemical and Engineering Aspects*, 2020, 595: 124508.
- [14] PARK K, PARK S, CHOI J, KIM G, TONG M, KIM H. Influence of excess sulfide ions on the malachite–bubble interaction in the presence of thiol-collector [J]. *Separation and Purification Technology*, 2016, 168: 1–7.
- [15] SOTO H, LASKOWSKI J. Redox conditions in the flotation of malachite with a sulphidizing agent [J]. *Mineral Processing and Extractive Metallurgy*, 1973, 82: c153–c157.
- [16] FENG Qi-cheng, ZHAO Wen-juan, WEN Shu-ming, CAO Qin-bo. Copper sulfide species formed on malachite surfaces in relation to flotation [J]. *Journal of Industrial and Engineering Chemistry*, 2017, 48: 125–132.
- [17] GUSH J C D. Flotation of oxide minerals by sulphidization—The development of a sulphidization control system for laboratory testwork [J]. *Journal of the South African Institute of Mining and Metallurgy*, 2005, 105: 193–197.
- [18] FENG Qi-cheng, WEN Shu-ming, DENG Jiu-shuai, ZHAO Wen-juan. Combined DFT and XPS investigation of enhanced adsorption of sulfide species onto cerussite by surface modification with chloride [J]. *Applied Surface Science*, 2017, 425: 8–15.
- [19] ZHANG L. Electrochemical equilibrium diagrams for sulphidization of oxide copper minerals [J]. *Minerals Engineering*, 1994, 7(7): 927–932.
- [20] CASTRO S, SOTO H, GOLDFARB J, LASKOWSKI J. Sulphidizing reactions in the flotation of oxidized copper minerals. II: Role of the adsorption and oxidation of sodium sulphide in the flotation of chrysocolla and malachite [J]. *International Journal of Mineral Processing*, 1974, 1(2): 151–161.
- [21] LIU Rui-zeng, LIU Dian-wen, LI Jia-lei, LI Jiang-li, LIU Zhi-cheng, JIA Xiao-dong, YANG Sheng-wang, NING Shuai. Sulfidization mechanism in malachite flotation: A heterogeneous solid–liquid reaction that yields Cu_xS_y phases grown on malachite [J]. *Minerals Engineering*, 2020, 154: 106420.
- [22] ZHOU R, CHANDER S. Kinetics of sulfidization of malachite in hydrosulfide and tetrasulfide solutions [J]. *International Journal of Mineral Processing*, 1993, 37(3): 257–272.
- [23] WU Dan-dan, MAO Ying-bo, DENG Jiu-shuai, WEN Shu-ming. Activation mechanism of ammonium ions on sulfidation of malachite (201) surface by DFT study [J]. *Applied Surface Science*, 2017, 410: 126–133.
- [24] SMART R S C, JASIENIAK M, PRINCE K E, SKINNER W M. SIMS studies of oxidation mechanisms and

- polysulfide formation in reacted sulfide surfaces [J]. Minerals Engineering, 2000, 13(8): 857–870.
- [25] CONTINI G, LAAJALEHTO K, SUONINEN E, MARABINI A M. 5-Methyl-2-mercaptobenzoxazole adsorbed onto chalcocite (Cu_2S): An XPS and X-AES study [J]. Journal of Colloid and Interface Science, 1995, 171(1): 234–239.
- [26] LIU Jian, EJTEMAEI M, NGUYEN A V, WEN Shu-ming, ZENG Yong. Surface chemistry of Pb-activated sphalerite [J]. Minerals Engineering, 2020, 145: 106058.
- [27] MOULDER J F, CHASTAIN J, KING R C. Handbook of x-ray photoelectron spectroscopy: A reference book of standard spectra for identification and interpretation of XPS data [J]. Chemical Physics Letters, 1992, 220(1): 7–10.
- [28] HAN Guang, WEN Shu-ming, WANG Han, FENG Qi-cheng. Enhanced sulfidization flotation of cuprite by surface modification with hydrogen peroxide [J]. Transactions of Nonferrous Metals Society of China, 2021, 31(11): 3564–3578.
- [29] CABRERA-GERMAN D, GARCÍA-VALENZUELA J A, MARTÍNEZ-GIL M, SUÁREZ-CAMPOS G, MONTIEL-GONZÁLEZ Z, SOTELO-LERMA M, COTA-LEAL M. Assessing the chemical state of chemically deposited copper sulfide: A quantitative analysis of the X-ray photoelectron spectra of the amorphous-to-covellite transition phases [J]. Applied Surface Science, 2019, 481: 281–295.
- [30] FOLMER J C W, JELLINEK F. The valence of copper in sulphides and selenides: An X-ray photoelectron spectroscopy study [J]. Journal of the Less Common Metals, 1980, 76(1): 153–162.
- [31] PATTRICK R A D, MOSSELMANS J F W, CHARNOCK J M, ENGLAND K E R, HELZ G R, GARNER C D, VAUGHAN D J. The structure of amorphous copper sulfide precipitates: An X-ray absorption study [J]. Geochimica et Cosmochimica Acta, 1997, 61(10): 2023–2036.
- [32] BUCKLEY A, WOODS R. An X-ray photoelectron spectroscopic study of the oxidation of chalcopyrite [J]. Australian Journal of Chemistry, 1984, 37(12): 2403–2413.
- [33] CHEN Xu-meng, PENG Yong-jun, BRADSHAW D. The separation of chalcopyrite and chalcocite from pyrite in cleaner flotation after regrinding [J]. Minerals Engineering, 2014, 58: 64–72.
- [34] QIU Xiao-bin, WEN Jian-kang, HUANG Song-tao, YANG Hong-ying, LIU Mei-lin, WU Bao. New insights into the extraction of invisible gold in a low-grade high-sulfur Carlin-type gold concentrate by bio-pretreatment [J]. International Journal of Minerals, Metallurgy, and Materials, 2017, 24(10): 1104–1111.
- [35] SMART R, SKINNER W, GERSON A. XPS of sulphide mineral surfaces: Metal-deficient, polysulphides, defects and elemental sulphur [J]. Surface and Interface Analysis, 1999, 28: 101–105.

氧气和硫化钠对赤铜矿浮选的影响及作用机理

贾晓东^{1,2}, 宋凯伟^{1,2}, 蔡锦鹏^{1,2}, 苏超^{1,2}, 徐晓会³, 马印禹⁴, 申培伦^{1,2}, 刘殿文^{1,2}

1. 昆明理工大学 省部共建复杂有色金属资源清洁利用国家重点实验室, 昆明 650093;
2. 昆明理工大学 云南省战略金属矿产资源绿色分离与富集重点实验室, 昆明 650093;
3. 华北理工大学 研究生院, 唐山 063210; 4. 山东黄金集团有限公司, 济南 250100

摘要: 通过浮选试验、场发射扫描电子显微镜(FESEM)、电子探针(EPMA)以及X射线光电子能谱(XPS)等研究氧气和硫化钠对赤铜矿浮选的影响。浮选试验表明, 用适量的硫化钠预处理赤铜矿表面后可大幅提升赤铜矿的可浮性。FESEM显示硫化后的赤铜矿表面覆盖有大量碎片, 在 Na_2S 浓度为 5.0×10^{-4} mol/L时, 这些碎片的形状更加规则和完整。结合EPMA和EDS分析发现, 这些碎片是新形成的铜硫化物, 是促进赤铜矿高效浮选的关键。XPS分析表明, 赤铜矿暴露于空气中表面极易被氧化成 CuO , 硫化钠优先与表面的 CuO 膜发生氧化还原反应, 此过程中, Cu^{2+} 被还原为 Cu^+ , S^{2-} 主要被氧化为 $(\text{S}_2)^{2-}$ 和 $(\text{S}_n)^{2-}$ 。

关键词: 赤铜矿; 硫化浮选; 硫化机理; 氧化; 硫化铜

(Edited by Bing YANG)